ACS chemical biology

ARTICLES

pubs.acs.org/acschemicalbiology

The Antimalarial Ferroquine: Role of the Metal and Intramolecular Hydrogen Bond in Activity and Resistance

Faustine Dubar,[†,+] Timothy J. Egan,[‡,*] Bruno Pradines,[§] David Kuter,[‡] Kanyile K. Ncokazi,[‡] Delphine Forge,[∥] Jean-François Paul,[†] Christine Pierrot,[¶] Hadidjatou Kalamou,[¶] Jamal Khalife,[¶] Eric Buisine,[⊥] Christophe Rogier,[§] Hervé Vezin,[#] Isabelle Forfar,[▽] Christian Slomianny,[○] Xavier Trivelli,[+] Sergey Kapishnikov,[◆] Leslie Leiserowitz,[◆] Daniel Dive,[¶] and Christophe Biot[†,+,*]

[†]Université de Lille1, Unité de Catalyse et Chimie du Solide - UMR CNRS 8181, ENSCL, Bâtiment C7, B.P. 90108, 59652 Villeneuve d'Ascq Cedex, France

[‡]Department of Chemistry, University of Cape Town, Private Bag, Rondebosch 7701, South Africa

[§]Institut de Recherche Biomédicale des Armées, Antenne de Marseille, Unité de Recherche en Biologie et Epidémiologie Parasitaires, URMITE -UMR 6236, Allée du Médecin Colonel Jamot, Parc le Pharo, BP 60109, 13262 Marseille Cedex 07, France

[∥]Laboratoire de chimie organique, Université de Mons, 20 place du parc, 7000 Mons, Belgium

[⊥]Ecole Nationale Supérieure de Chimie de Lille, Bâtiment C7, Avenue Mendeleïev - B.P. 90108, 59652 Villeneuve d'Ascq cedex, France

[#]Université de Lille1, Laboratoire de Spectrochimie Infrarouge et Raman (LASIR), CNRS UMR 8516, Bâtiment C4, 59655 Villeneuve d'Ascq Cedex, France

[▽]Université de Bordeaux, Pharmacochimie EA 4138, Bordeaux, France

[○]Université de Lille1, Inserm U1003 - Laboratoire de Physiologie Cellulaire, Bâtiment SN3, 59655 Villeneuve d'Ascq Cédex, France

[◆]Department of Materials and Interfaces, Weizmann Institute of Science, 76100 Rehovot, Israel

[¶]CIIL, Inserm U 1019, UMR CNRS 8024 Université Lille Nord de France, Institut Pasteur de Lille, 1 rue du Pr Calmette, 59019 Lille Cedex, France

[+]Université de Lille1, Unité de Glycobiologie Structurale et Fonctionnelle, CNRS UMR 8576, IFR 147, 59650 Villeneuve d'Ascq Cédex, France

Supporting Information

ABSTRACT: Inhibition of hemozoin biocrystallization is considered the main mechanism of action of 4-aminoquinoline antimalarials including chloroquine (CQ) but cannot fully explain the activity of ferroquine (FQ) which has been related to redox properties and intramolecular hydrogen bonding. Analogues of FQ, methylferroquine (Me-FQ), ruthenoquine (RQ), and methylruthenoquine (Me-RQ), were prepared. Combination of physicochemical and molecular modeling methods showed that FQ and RQ favor intramolecular hydrogen bonding between the 4-aminoquinoline NH group and the terminal amino group in the absence of water, suggesting that this structure may enhance its passage through the membrane. This was further supported by the use of Me-FQ and Me-RQ where the intramolecular hydrogen bond cannot be formed. Docking studies suggest that FQ can interact specifically with the {0,0,1} and {1,0,0} faces of hemozoin, blocking crystal growth. With respect to the structure−activity relationship, the antimalarial activity on 15 different *P. falciparum* strains showed that the activity of FQ and RQ were correlated with each other but not with CQ, confirming lack of cross resistance. Conversely, Me-FQ and Me-RQ showed significant cross-resistance with CQ. Mutations or copy number of *pfcrt*, *pfmrp*, *pfmdr1*, *pfmdr2*, or *pfnhe-1* did not exhibit significant correlations with the IC_{50} of FQ or RQ. We next showed that FQ and Me-FQ were able to generate hydroxyl radicals, whereas RQ and me-RQ did not. Ultrastructural studies revealed that FQ and Me-FQ but not RQ or Me-RQ break down the parasite digestive vacuole membrane, which could be related to the ability of the former to generate hydroxyl radicals.

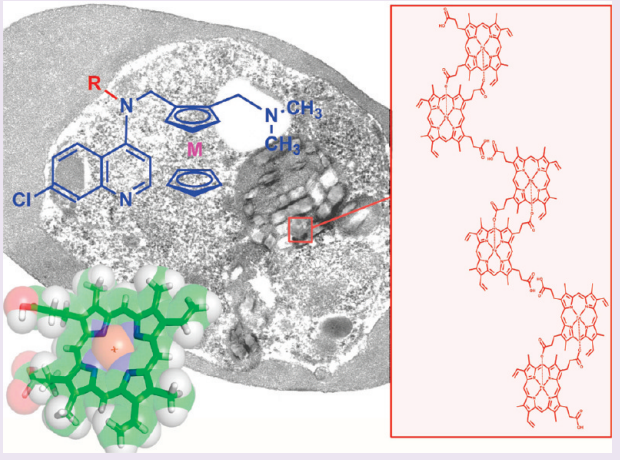

Received: October 13, 2010
Accepted: December 16, 2010
Published: December 16, 2010

Widespread occurrence of strains of *Plasmodium falciparum* resistant to chloroquine (CQ, Chart 1) and the antifolate combination of sulfadoxine/pyrimethamine has led to the introduction of artemisinin combination therapy (ACT).[1] ACT is now the WHO recommended treatment of uncomplicated malaria.[2] The treatment currently involves a combination of an artemisinin derivative (*i.e.*, artemether or artesunate) and a quinoline or related arylmethanol derivative (*i.e.*, mefloquine (MQ), amodiaquine (AQ), or lumefantrine). However, recent fears of the emergence of artemisinin resistance in Cambodia[3] highlight the need for ongoing development of new weapons against malaria. Previous studies by us and others have shown that aminoquinolines with side chains including a metallocene are active against CQ-resistant *P. falciparum*.[4] Evaluation of about 120 derivatives yielded ferroquine (FQ, SSR97193, Chart 1). FQ in association with artesunate has progressed to phase IIb clinical trials.[5] During our initial work on the mechanism of action of FQ, we pointed out the possible contribution to antimalarial activity of the redox properties of the ferrocene/ferricinium system[6] and of intramolecular hydrogen bonding in the lateral side chain of FQ.[7] In the present work, we designed and synthesized new compounds specifically to probe the relevance of these two hypotheses. Replacement of iron(II) in FQ with ruthenium(II) in ruthenoquine (RQ) should prevent the redox reaction, and the presence of a methyl group on the 4-amino group in methyl ferroquine (Me-FQ) and methyl ruthenoquine (Me-RQ) should prevent the formation of the intramolecular hydrogen bond. For these four molecules, FQ, RQ, Me-FQ, and Me-RQ, we compared the properties considered important for antimalarial activity: (i) the influence of structure on lipophilicity, (ii) the role of heme binding, and (iii) the noncovalent interactions with hemozoin. We also assessed the *in vitro* activity of the four molecules FQ, RQ, Me-FQ, and Me-RQ against 15 strains of *P. falciparum* from a wide panel of countries and with different susceptibility profiles. We next evaluated whether the effects of these different compounds are correlated among each other and with other already known antimalarials (*i.e.*, exhibit cross-resistance) and/or with clones that are related to mutations or copy number of genes involved in quinoline resistance, that is, *pfcrt* (*Plasmodium falciparum* chloroquine resistance transporter) coding PfCRT,[8] *pfmdr1* (*P. falciparum* multidrug resistance 1) coding PfMDR1 or Pgh1,[9,10] *pfmdr2* (*P. falciparum* multidrug resistance 2) (coding PfMDR2),[11] *pfmrp* (*P. falciparum* multidrug resistance-associated protein) coding PfMRP1,[12] or *pfnhe-1* (*P. falciparum* Na^+/H^+ exchanger) coding PfNHE.[13] All of these studies provide new insight into how FQ acts against the parasite.

Chart 1. Compounds Investigated in This Study: Chloroquine (CQ), Ferroquine (FQ), Methylferroquine (Me-FQ), Ruthenoquine (RQ), and Methylruthenoquine (Me-RQ)

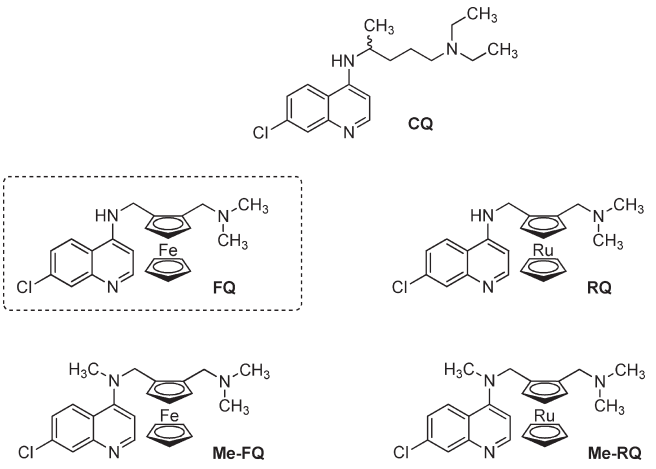

RESULTS AND DISCUSSION

Synthesis. The compounds investigated in this study are presented in Chart 1. Note that the synthesis of FQ,[14] Me-FQ,[7] and RQ[15] have been previously reported by ourselves and others. Me-RQ was obtained according to a similar procedure as Me-FQ (Supporting Information S2).[7] For RQ, we did not apply the synthesis reported by Beagley *et al.*[15] but rather used a modified synthesis of ruthenocene (Supporting Information S2) with similar methodology developed for the synthesis of FQ.[14]

Intramolecular Hydrogen Bonding Properties. A possible explanation for the enhanced activity of FQ and its analogues relative to CQ is that these compounds exhibit more lipophilic character.[16] In addition, the observation of an intramolecular hydrogen bond between the unprotonated terminal tertiary amino group and the 4-amino group of the quinoline in the crystal structure of RQ suggests that adoption of such a folded conformation enhances transport of these drugs through membranes because the folded conformation would be expected to be more lipophilic than the open conformation. As a first step to probing this hypothesis, conformational analysis was carried out on the four molecules FQ, RQ, Me-FQ, and Me-RQ with density functional theory (DFT) calculations (RPBE)[17,18] using the valence triple-ζ plus polarization basis set TZVP.[19] In vacuum, the minimum-energy conformation in the neutral FQ and RQ evidenced the presence of the intramolecular hydrogen bond between N11 and N24 (Figure 1a and Supplementary Figure SI1) as experimentally observed in their crystal structures. The intramolecular hydrogen bond is slightly stronger in FQ than in RQ, the energy difference between them being 1.4 kcal/mol. The presence of the methyl groups in Me-FQ and Me-RQ has an impact on the orientation of the amino side chain with respect to the quinoline ring. Here the minimum-energy conformation was obtained for H3 close to H27 (Figure 1b). Compared to FQ (and RQ), the bulky ferrocenyl group is twisted around the bond between N11 and C4 to minimize the steric and electronic interactions with the quinoline ring. Shape analysis was achieved by computing the molecular electrostatic potential (MEP) surfaces of the compounds (Figure 1c and d). The polar surface areas (PSA) were estimated at 14 $Å^2$ for FQ and only 10 $Å^2$ for Me-FQ. Thus, computational analysis suggests that FQ and RQ are likely to exhibit an intramolecular hydrogen bond (at least in low dielectric media).

To experimentally verify the predictions of the computational studies, solution NMR experiments were done. For neutral RQ, resonances of N24 and H11 were correlated in the ^{15}N-HMBC NMR experiment, demonstrating the presence of an intramolecular hydrogen bond in low dielectric constant solution ($CDCl_3$). Moreover, NOESY experiments confirm that neutral RQ adopts a folded conformation. This special conformation was evidenced by the presence of NOEs between H5 and the terminal methyl groups and H3 and the H12 and the absence of NOEs between H5 and H12, and H3 and H(N11). NOESY experiments were also carried out in d_5-pyridine at lower concentration and higher temperature (343 K) at 400 MHz. Under these experimental

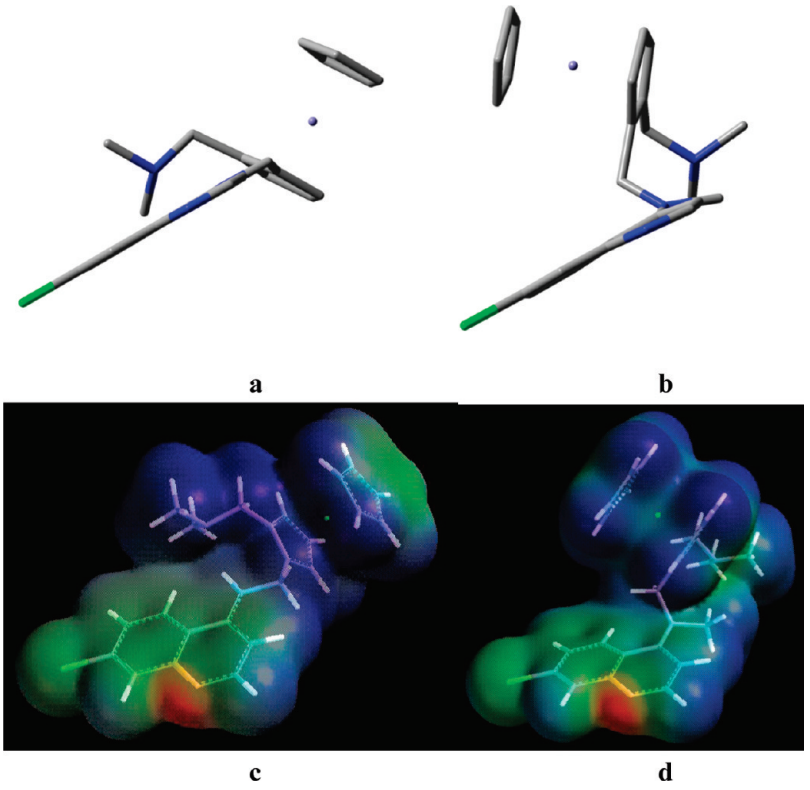

Figure 1. Structural features of FQ and Me-FQ based on computational chemistry. Minimum energy conformations for FQ (a) and Me-FQ (b) calculated at the RPBE/TZVP level of theory. Molecular electrostatic potentials for FQ (c) and Me-FQ (d).

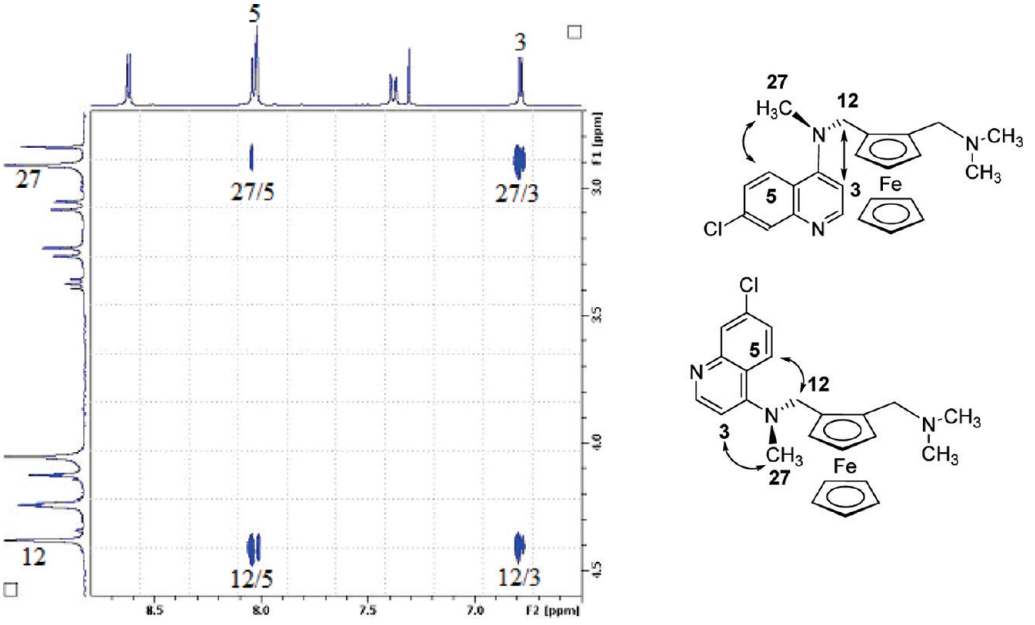

Figure 2. NOESY spectra of Me-FQ and the corresponding conformations of Me-FQ.

conditions, no difference in the NOESY spectra can be observed, confirming that the observed NOEs were intramolecular and not intermolecular. This folded conformation is not observed for diprotonated FQ in D_2O. ROESY experiments confirm that diprotonated FQ has no fixed conformation. Only ROEs between H3 and H12 as well as between H5 and H12 were observed (Figure 2).

On the other hand, Me-FQ and Me-RQ are not able to establish an intramolecular hydrogen bond and are not expected to adopt a fixed conformation. The complete assignment of the ^1H and ^{13}C solution NMR signals of Me-FQ and Me-RQ were achieved on the basis of COSY, ^{13}C-HSQC, ^{13}C-HMBC, and NOESY experiments. Taking Me-FQ as an example, in $CDCl_3$, NOEs between H5 (δ = 8.05 ppm) and H27 (δ = 2.91 ppm),

dx.doi.org/10.1021/cb100322v |*ACS Chem. Biol.* 2011, 6, 275–287

Table 1. ^{15}N Chemical Shifts of the Quinoline N (N1), 4-Amino N (N11), and Side Chain N (Nsc) in FQ, Me-FQ, RQ, Me-RQ, and CQ

	FQ/Me-FQ			RQ/Me-RQ			CQ		
	N1	N11	Nsc	N1	N11	Nsc	N1	N11	Nsc
N11-H	263	84	35	263	85	35	263	90	45
N11-Me	279	61	31	279	60	30			
Cp-CH_2-NMe_2			310			320			

between H3 (δ = 6.78 ppm) and H27, between H12 (δ = 4.40 ppm) and H5, and between H12 and H3 (Figure 2) show that the C4−N11 bond is not blocked (unlike FQ and RQ).

Nitrogen-15 chemical shifts have been indirectly determined in ^{15}N-HMBC experiments, which compensate the low sensitivity and natural abundance of this nucleus (Table 1). The five investigated compounds CQ, FQ, RQ, Me-FQ and Me-RQ can be separated in two groups. The hydrogen bond is observed in the first group (CQ, FQ, and RQ) and absent in the second group (Me-FQ and Me-RQ). These two groups show different ^{15}N chemical shifts patterns. The occurrence of the hydrogen bond leads to a shielding effect on ^{15}N1 (16 ppm) and a deshielding effect on ^{15}N11 (around 15 ppm) and ^{15}N from the side chain (around 5 ppm). These NMR experiments confirm the results of the computational study, demonstrating that FQ and RQ do indeed exhibit intramolecular hydrogen bonding in nonaqueous solvents.

Generation of Hydroxyl Radicals. Under oxidizing conditions, FQ has been reported to be able to undergo a Fenton-like reaction,[6] thereby yielding hydroxyl radicals (HO°):

$$\mathrm{FQ(II) + H_2O_2 \rightarrow FQ(III) + HO^- + HO^\circ}$$

EPR spin trapping experiments were carried out to determine whether RQ, Me-FQ, and Me-RQ undergo similar reactions. The spin trap agent used to observe the formation of HO° radicals was DMPO. Oxidizing conditions were induced by adding H_2O_2 solutions at two different concentrations, 1 and 15 mM, respectively. The latter has been claimed to be the concentration at which H_2O_2 is found in the digestive vacuole of the parasite.[20] In this respect, the pH in the food vacuole of the parasite being acidic (∼5), only the diprotonated species were tested for their ability to form radicals.

Only the EPR spectra of Me-FQ displayed a typical quartet with an intensity ratio of 1:2:2:1 and hyperfine splitting coupling constants, $a_H = a_N$ = 13.2 G (Figure SI2). These spectroscopic results unambiguously demonstrate the formation of the hydroxyl radical spin adduct DMPO−OH°. On the other hand, no signals were detected for RQ and Me-RQ. We conclude that ruthenocene derivatives are not able to generate the formation of HO° radicals.

The HO° radicals formed by diprotonated Me-FQ during the Fenton reaction were quantified by double integration of EPR spectra. 2,2,6,6-Tetramethylpiperidinyl-1-oxyl (TEMPO) was used as intensity reference at a concentration of 0.1 mM in methanol. A hydroxyl production of 0.6 and 3.5 μM was then measured for Me-FQ·2HCl in the presence of 1 and 15 mM H_2O_2, respectively. These results are in accordance with those obtained previously for FQ·2HCl.[6]

Electrochemical Behavior. We reported the redox behavior of neutral and diprotonated FQ.[6] As cyclic voltammetry of the ruthenium complexes was rendered complicated owing to electroprecipitation problems (data not shown), DFT calculations were performed to help in the understanding of the electrochemical behavior of neutral and diprotonated RQ. The energies of the various oxidation states were calculated using the B3LYP functional[21,22] and TZVP basis sets.[19] The results showed that diprotonated RQ exhibit higher resistance to electron loss than diprotonated FQ ($\Delta E_{1/2} = E_{1/2}(\mathrm{RQ}) - E_{1/2}(\mathrm{FQ}) = +0.92$ V).

Table 2. Partition Coefficients (log D), Acid Dissociation Constants (pK), Vacuolar Accumulation Ratios, and Hydroxyl Radical Production in FQ, Me-FQ, RQ, Me-RQ, and CQ

	log $D_{5.2}$	log $D_{7.4}$	pK_{a1}	pK_{a2}	VAR[a]	HO° production
CQ	−1.20	0.85	7.94	10.03	112	−
FQ	−0.77	2.95	7.00	8.45	5248	+
Me-FQ	−0.56	3.04	7.05	8.80	3981	+
RQ	−0.73	3.35	6.99	7.97	12022	−
Me-RQ	−0.04	3.60	7.18	9.20	4365	−

[a] Predicted from log D values.

Table 3. Percent Ionization of FQ, Me-FQ, RQ, Me-RQ, and CQ at pH 5.2 and 7.4

	% present at pH 5.2			% present at pH 7.4		
	2+[a]	1+[a]	0[a]	2+[a]	1+[a]	0[a]
CQ	100.00	0.00	0.00	99.70	0.23	0.07
FQ	99.94	0.06	0.00	76.16	6.79	17.05
Me-FQ	99.97	0.03	0.00	88.58	3.53	7.89
RQ	99.83	0.17	0.00	50.99	13.73	35.28
Me-RQ	99.99	0.01	0.00	95.96	1.52	2.52

[a] Charge.

Acid Dissociation Constants and Lipophilicity. To probe hydrophilicity/lipophilicity changes induced in the different compounds studied,[23] their distribution coefficients were measured in *n*-octanol−water mixtures at two pH values (5.2 and 7.4) relevant to vacuolar and cytosolic conditions, respectively (Table 2). The acid dissociation constants were also determined by potentiometry (Table 2), to calculate the ionization percentage by the Henderson−Hasselbach equation of the diprotonated, monoprotonated, and neutral forms of all compounds at the two characteristic pHs (Table 3). The degree of ionization controls permeability and solubility of the compounds.

All compounds display a strong hydrophilicity at vacuolar pH, being diprotonated in this pH range. At pH 5.2 lipophilicity follows the order Me-RQ > Me-FQ > RQ > FQ > CQ. At this pH the differences between the distribution values are very slight. The replacement of the iron atom in FQ by the ruthenium atom in RQ has no effect on the lipophilicity.

On the other hand, at pH 7.4, all compounds except CQ are significantly lipophilic. The lipophilicity trend at cytosolic pH is Me-RQ > RQ > Me-FQ > FQ. The replacement of Fe(II) in FQ and Me-FQ by Ru(II) in RQ and Me-RQ, respectively, increases the lipophilicity by about 3-fold. At pH 7.4, differences in the degree of ionization also need to be considered, because the two methylated compounds Me-FQ and Me-RQ exist only in the diprotonated form, while the nonmethylated derivates FQ and RQ exhibit significantly lower percentages of this form. The presence of the CH_3 donor group in Me-FQ and Me-RQ increases the pK_{a1} value (the acid dissociation constant of the quinolinium group) of both compounds.

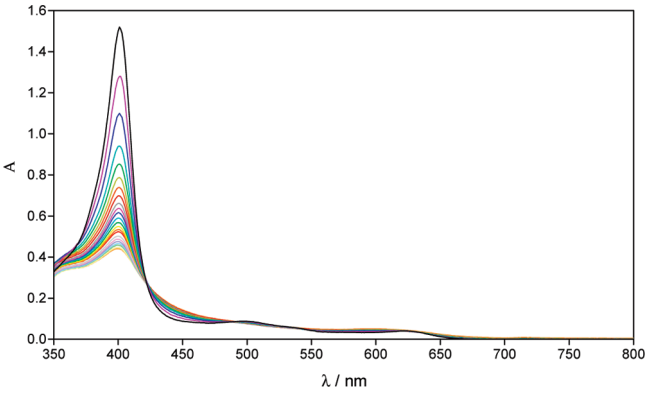

Figure 3. Typical spectrophotometric titration (dilution corrected) for Fe(III)PPIX with FQ. Data obtained in 40% aqueous DMSO (v/v), pH 7.4, 25 °C.

Table 4. Association Constants (log *K*) and Stoichiometry of Interaction between Hematin (Fe(III)PPIX) and CQ, FQ, RQ, Me-FQ, and Me-RQ Determined by Spectrophotometric Titration in 40% Aqueous DMSO (v/v), pH 7.4 and 25 °C

	log *K*	binding stoichiometry (ligand:Fe(III)PPIX)
CQ	5.52 ± 0.03	1:1
FQ	5.52 ± 0.03	1:1
Me-FQ	4.71 ± 0.03	1:1
RQ	4.44 ± 0.09	2:1
	4.47 ± 0.03	
Me-RQ	4.59 ± 0.01	1:1

The formation of an intramolecular hydrogen bond might be expected to increase the lipophilicity of the molecule. However, regardless of the pH of the medium, alkylation of the 4-amino in FQ and RQ increases the lipophilicity more than the presence of the intramolecular hydrogen bond.

Finally, vacuolar accumulation ratios were estimated from the measured log *D* values according to eq 1 (Table 2).

$$\mathrm{VAR} = \mathrm{antilog}(\log D_{7.4} - \log D_{5.2}) \qquad \text{(eq 1)}$$

The VAR value calculated from experimental log *D* values are surprisingly more than 2 orders of magnitude lower than those predicted using the Henderson−Hasselbach equation in the case of CQ (19,532 vs 112) but relatively similar in the case of FQ, Me-FQ, RQ, and Me-RQ, which differ by a factor of at most a little more than 2-fold. In the case of CQ, the reason for the discrepancy is that the log *D* value of the diprotonated form at pH 5.2 is considerably higher than expected (calculated log $D_{5.2}$ = −2.85, a 45-fold difference).

Association of Hematin with FQ, RQ, Me-FQ, and Me-RQ. The Soret band of hematin at 402 nm was monitored as a function of FQ, RQ, Me-FQ, and Me-RQ concentration after correction for dilution and for absorbance by the respective compounds at this wavelength. Figure 3 shows a typical set of absorbance spectra. Fitting of the data to a 1:1 association model yielded the association constants for FQ, Me-FQ, and Me-RQ (Figure 3 and Table 4). Interestingly, we found a higher binding constant for FQ than we reported previously.[23] This value is exactly the same as for CQ. In fact, the log *K* value of FQ decreases with time (data not shown), suggesting that FQ is altered in solution over a period

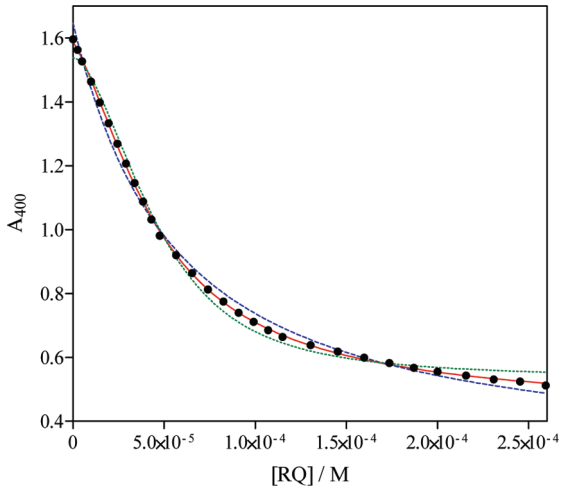

Figure 4. Nonlinear least-squares fits of experimental data obtained from spectrophotometric titration of Fe(III)PPIX with RQ. Models to which the data are fitted are 1:1 (dashed blue line), 2:1 stepwise (solid red line), and 2:1 one-step (dotted green line). Conditions as in Figure 3.

of hours. These changes could be a result either of aggregation or oxidation of FQ. The latter hypothesis is in accordance to our recent observations. Indeed, we have postulated that the redox behavior of FQ could be responsible for destruction of the hematin-drug complex by a Fenton-like reaction.

In the case of Me-FQ and Me-RQ, log *K* values are lower than that of FQ, but still in a similar range (Table 4). It would appear that the presence of the methyl group alters the specificity and geometry of interaction between the drugs and hematin, leading to a decrease in the association constants.

RQ is the only compound to give a different binding stoichiometry. The data indicate a 2:1 stepwise association (Figure 4). It is clear from this figure that the observed association isotherm deviates from both the 1:1 model and 2:1 one-step model but conforms very well to the 2:1 stepwise model. The association constants are also lower than that of FQ. This difference may arise from the larger molecular volume of RQ (350 cm^3/mol) compared to FQ (280 cm^3/mol).

Interestingly, although RQ associates with hematin more weakly than FQ, it is expected to accumulate more strongly (according to the VAR values reported in Table 1). These two contributions to the antimalarial activity might compensate for one another since RQ is equally active *in vitro* as FQ (see below). On the other hand, Me-FQ and Me-RQ with weaker log *K* values than FQ but with similar VAR values are both substantially less active against parasites. These data suggest that other factors are implicated in the antimalarial activity.

Proposed Binding Sites of Ferroquine on Hemozoin Crystal Faces. The inhibition of nucleation and/or growth of hemozoin crystals as induced by FQ may be explained by the stereoselective binding of FQ to the principle faces thereof. Both the biogenic and synthetic forms of hemozoin generally display three dominant faces of a needle-shaped crystal: the {*h*,*k*,*l*} side faces {1,0,0} and {0,1,0}, which are almost at right angles to each other, and the {0,1,1} face, which is slanted with respect to the needle *c*-axis, terminating the crystal at either end.[24] Crystals of biogenic hemozoin sometimes display {0,0,1} end faces, which are almost perpendicular to the *c*-axis and generally not well developed. The {0,0,1} face, which is highly corrugated, exposes the propionic acid moiety $CH_2CH_2CO_2H$, the propionate group O=

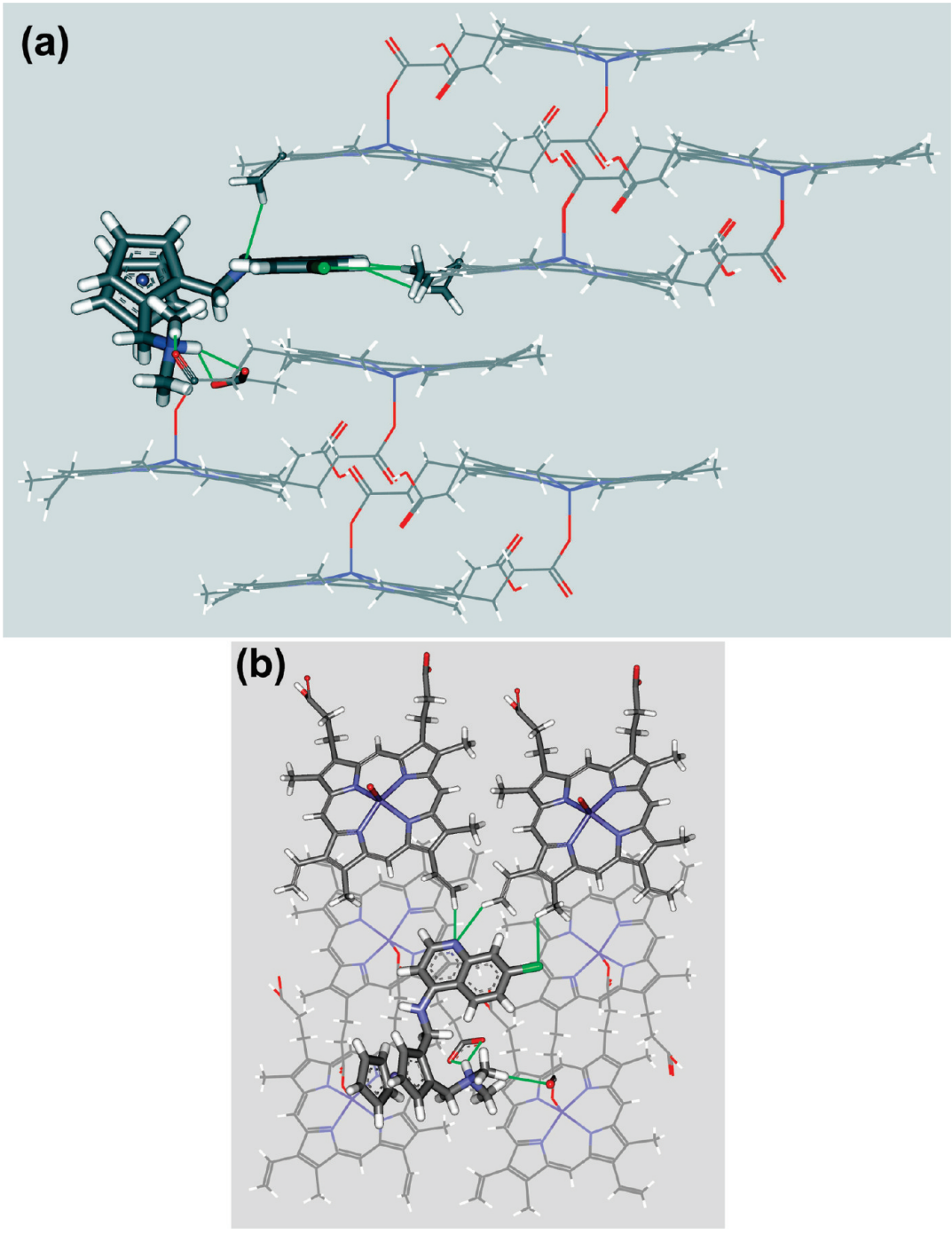

Figure 5. FQ bound to the {0,0,−1} face of a synthetic hemozoin crystal highlighting energetically favorable interactions. Views: (a) the crevice along the *a*-axis within which the drug is intercalated; (b) along a general direction. The following distances (in Å, highlighted in green) are between atoms **N**$(CH_3)_2$H···$\mathbf{O_2}$C 2.9, 2.9; N$\mathbf{CH_3}$···**O**=COFe 3.3; **Cl**···$\mathrm{H_3}$**C** 3.7; (aromatic)**N**···H**C**(=CH) 3.7, 3.9; (aromatic)C−**N**···H**C**=CH 3.3.

C−O−Fe, ring peripheral C−H groups, and part of the plane of the heme ring. The {1,0,0} face exposes, but at an oblique angle, the $CH_2CH_2CO_2H$ acid group and ring peripheral C−H groups, whereas the side face {0,1,0} exposes the plane of the heme ring.

To retard nucleation/growth of hemozoin, an antimalarial drug should bind to at least the needle end faces {0,0,1} or {0,1,1}. An effective inhibitor of crystal nucleation/growth of hemozoin should also bind to either the {1,0,0} or {0,1,0} faces. The proposed mechanism of action of CQ involves binding to the {0,0,1} and {1,0,0} faces.[25] Note that although the {0,0,1} face is generally poorly expressed, it may form ledges on the {0,1,1} face, as induced by adsorption of the drug onto {0,0,1} molecular surface sites.

To fix the conformation of FQ so that it may be adsorbed onto the {0,0,1} and {1,0,0} faces, the adsorbate was adjusted to adopt a conformation as close as possible to CQ adsorbed onto the {0,0,1} and {1,0,0} faces. The conformational energy of FQ was then minimized with the COMPASS force field. The binding energy of FQ to the {0,0,1} and the {1,0,0} faces was minimized but maintaining rigid structures of the molecular surface sites of

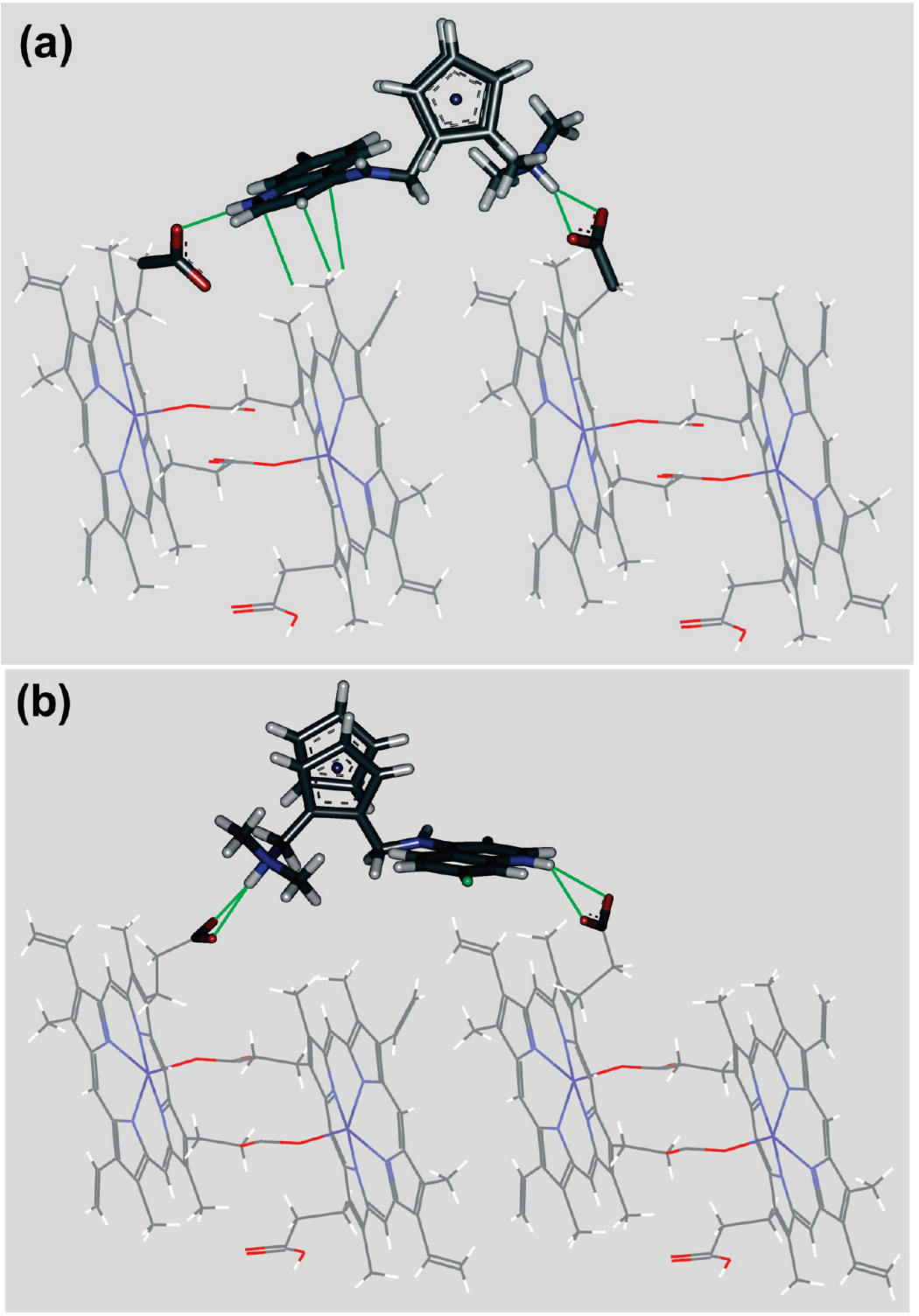

Figure 6. Intermolecular contacts between FQ and synthetic hemozoin at the {1,0,0} crystal surface. Views edge-on to the plane of the {1,0,0} face. The following distances (in Å, highlighted in green) are between atoms: (a) **N**$(CH_3)_2$H···**O**$_2$C 2.9, 2.9; (aromatic)**N**···**O**$_2$C 3.1; center of N-containing ring···H_3**C** 3.3. (b) **N**$(CH_3)_2$H···**O**$_2$C 3.3, 3.3; (aromatic)**N**··· **O**$_2$C 3.2, 3.2.

hemozoin. The conformations of the propionic acid moieties, relevant vinyl -C═CH_2 and methyl CH_3 groups of the host crystal exposed at the {0,0,1} and {1,0,0} faces were then adjusted manually to best satisfy acid−base N−H···O and C−H···X (O or N) hydrogen bond geometries between adsorbate and the crystal surface.

The proposed binding arrangements of FQ bound to the {0,0,1} and {1,0,0} crystal surfaces of synthetic hemozoin are depicted in Figures 5 and 6. FQ stereochemically caps the {0,0,1} surface *via* the exocyclic tertiary amine···acid salt bridge and still fits snugly on that surface, by intercalation of the quinoline rings between the heme rings of the hemozoin molecules,

dx.doi.org/10.1021/cb100322v |*ACS Chem. Biol.* 2011, 6, 275–287

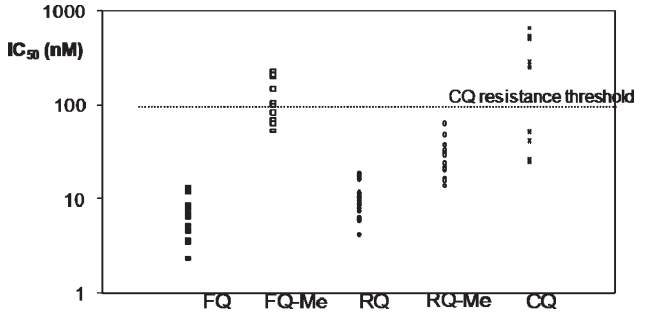

Figure 7. *In vitro* antimalarial activity of CQ, FQ, RQ, Me-FQ, and Me-RQ against 15 susceptible and resistant parasite strains.

FQ also form C−Cl···H_3C and (quinoline ring)N···HC═C(vinyl) hydrogen bonds, albeit weak, with the heme surface molecule to help anchor the guest within the crevice (Figure 5). For effective binding of FQ to the {1,0,0} face, advantage is taken of the flexibility of the propionic acid chains coupled with the approximate match in distance between translated-related propionic acid groups along the *b*-axis of hemozoin (14.7 Å) and between the terminal N atom and the quinoline ring N atom of FQ (8.9 Å) plus two NH···O distances of ∼3 Å each. By such means it is possible to form acid−base N−H···O bonds between a diprotonated FQ molecule and charged CO_2 groups of hemozoin (Figure 6).

Correlations of *in Vitro* Antimalarial Activity. Fifteen *P. falciparum* strains were tested for their *in vitro* susceptibility to CQ, FQ, Me-FQ, RQ, and Me-RQ (Figure 7 and Table SI1). The geometric mean IC_{50} values and 95% confidence interval are 6.4 nM (4.9−8.4) for FQ, 126.4 nM (94−170) for Me-FQ, 9.2 nM (7.2−11.6) for RQ, 26.1 nM (20.6−33.0) for Me-RQ, and 157 nM (76−325) for CQ. The difference between FQ and RQ was significant (p-value = 0.0007). Indeed, all of the differences between the responses of the 5 compounds were significant ($0.0007 < p\text{-value} < 0.0468$).

In vitro cross-resistance was measured by pairwise correlation of IC_{50} values of all 15 strains (Table SI2). A significant positive correlation was found between responses to FQ and RQ, between FQ and Me-RQ, Me-FQ and CQ, and between RQ and Me-RQ (Table SI2). A positive correlation between the IC_{50} values of two antimalarial drugs may suggest *in vitro* cross-resistance or at least common mechanisms of action; however, the relationship between *in vitro* and *in vivo* resistance depends on the level of resistance and the coefficients of correlation (r) and determination (r^2). To suggest the same mechanism of action or resistance (which could induce cross-resistance) for two compounds, the coefficient of determination must be high, such as the one for FQ and RQ ($r^2 = 0.96$). Variations in the response to FQ or RQ are not explained by variation in the response to CQ.

Correlations with Gene Mutations in Proteins Associated with Drug Resistance. After Bonferroni correction, we did not find a significant association between FQ IC_{50} and polymorphism in *pfcrt*, *pfmdr1*, *pfmdr2*, *pfmrp*, or *pfnhe-1* number of *pfmdr1* gene copy (Table SI3). Significant associations were found between responses to CQ and polymorphism in *pfcrt* and *pfmrp* (Table SI3). The CQ geometric mean was 37 ± 13 nM for wild type 76*pfcrt* or wild type *pfmrp* and 451 ± 146 nM for mutant 76*pfcrt* and mutant *pfmrp*. The associations between CQ IC_{50} and ms4760 profiles, number of DNNND or DDDNHNDNHNN repeats, and *pfmdr1* copy number were not significant after Bonferroni correction. There was no significant association between RQ IC_{50} or Me-RQ and polymorphisms in *pfcrt*, *pfmdr1*, *pfmdr2*, *pfmrp*, *pfnhe-1*, or gene copy number of *pfmdr1*. The associations between Me-FQ IC_{50} and *pfcrt*, *pfmrp*, *pfmdr1*, *pfmdr2*, number of DNNND or DDDNHNDNHNN repeat, and *pfmdr1* copy number were significant before but not after Bonferroni correction.

Table 5. Cytotoxicity of CQ, FQ, RQ, Me-FQ, and Me-RQ in Adherent 3T6 cells

	IC_{50} (μM)
FQ	1.06 ± 0.01
Me-FQ	8.58 ± 0.07
RQ	1.49 ± 0.08
Me-RQ	11.55 ± 0.06

Curative Effect on Mice Infected with *P. vinckei vinckei* Strains. We used a CQ-resistant model previously described, in which mice should die at an early stage, with high levels of parasitemia.[26] Untreated infected mice died between days 6−9. Compounds were given subcutaneously at a dose of 10 mg/kg/d for 4 days. In contrast to FQ, which cured all animals infected with CQ-resistant *P. vinckei vinckei* strains at a dose 8.4 mg/kg/d for 4 days,[27] Me-FQ, RQ, and Me-RQ were unable to cure the infected mice. Parasitemia in RQ-treated mice reached 15% on day 4, and death occurred within the following 4 days. A similar observation was made for Me-FQ-treated mice; parasitemia reached 15% on day 4, and mice died between days 6−7. The mice treated with Me-RQ were the most parasitized (24% at day 4), and all died at day 7.

Cytotoxicity. All of the compounds exhibit relatively weak cytotoxicity against adherent mouse fibroblast 3T6 cells (Table 5), but the methylated derivatives are almost an order of magnitude less cytotoxic. FQ exhibits the highest cytotoxicity, while Me-RQ is least cytotoxic. However, owing to the weak antimalarial activity of Me-FQ, this compound exhibits the lowest selectivity index (SI). For example, the SI (IC_{50}(3T6)/IC_{50}(3D7)) is 83.3 for Me-FQ, 248 for RQ, 303 for FQ, and 696 for Me-RQ.

Ultrastructural Effects. Parasites treated by the four compounds (40 nM, 1 h) were examined by transmission electron microscopy (Figure 8). The main differences were observed at the level of the digestive vacuole, as expected from their supposed accumulation in this organelle and their possibility to produce hydroxyl radicals. The control culture shows a normal well-delineated digestive vacuole containing hemozoin crystals (Figure 8A). In parasites treated by FQ, crystals are observed bunched or dispersed in the cytoplasm, where they are in direct contact with cytosol components, and in most parasites, the digestive vacuole membrane is not visible (Figure 8B). In parasites treated with RQ, the digestive vacuole is well preserved, with total integrity of its membrane (Figure 8C). Me-FQ exerts a weaker effect than FQ, some parasites showing preliminary alterations (Figure 8D), while others have an intact digestive vacuole membrane (Figure 8E). In Me-RQ treated parasites, the digestive vacuole membrane has preserved its integrity (Figure 8F). Although crystals show resemblance in form (Figure 8A, B, and E), for the FQ-treated parasites the hemozoin crystals are exceptionally thin (50 nm), whereas the crystals grown without drug (control) or in the presence of RQ are much thicker (90−110 nm). No significant alterations were observed at the level of nucleus or mitochondria in treated parasites compared to control (not shown).

The aim of this paper is to provide a better understanding of the mechanism of action of FQ that could be used for the design

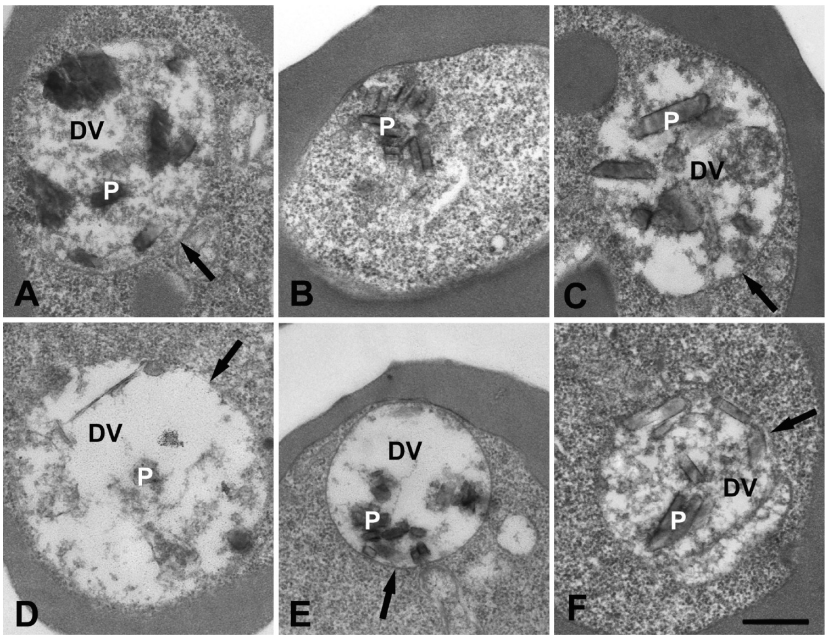

Figure 8. Ultrastructural effects of the four compounds on the HB3 strain of *P. falciparum*. Drug-treated (40 nM) and control parasites after one hour. (A) Control; (B) FQ; (C) RQ; (D, E) Me-FQ; (F) Me-RQ. DV: digestive vacuole. P: malarial pigment. Arrows indicate when DV membrane is conserved. The scale bar corresponds to 200 nm.

of new antimalarials. Hence, three analogues of FQ (Me-FQ, RQ, and Me-RQ) were specifically designed and synthesized, and the relationships between their structure, physicochemical properties, and biological activities were established. The methylation of the 4-amino group allows us to probe the importance of the intramolecular H-bond in the lateral side chain of FQ. The contribution of redox properties of the ferrocene/ferricinium system and the role of the metal ion were studied by replacement of the iron atom by a ruthenium atom. In view of the known mechanism of action of CQ, the role of heme binding and the inhibition of hemozoin formation were also investigated. Additional objectives were (i) to assess their *in vitro* activity against strains of *P. falciparum* with different susceptibility profiles, (ii) to evaluate whether the effects are correlated (that is, exhibit cross-resistance), and (iii) to evaluate whether their biological activities are related to mutations or copy number of genes involved in quinoline resistance.

Concerning the redox properties, the most striking difference between FQ and Me-FQ and RQ and Me-RQ is the inability of the Ru(II) complexes to generate hydroxyl radicals. In this regard, it is noteworthy that the redox properties of ferrocene and ruthenocene differ markedly. For many years it was assumed that while ferrocene readily undergoes one electron oxidation, ruthenocene undergoes only two electron oxidation to yield a Ru(IV) product.[28] Although it has been shown that the Ru(III) complex is formed, this complex is exceptionally susceptible to nucleophilic attack and results in formation of the Ru(IV) product.[28] Our present DFT calculations show that diprotonated RQ exhibits higher resistance to electron loss ($\Delta E_{1/2} = +0.92$ V) than diprotonated FQ. These differences in redox chemistry may account for the lack of hydroxyl radical formation by RQ and Me-RQ.

Concerning the intramolecular H-bond, combined theoretical calculations and NMR experiments clearly demonstrate that an intramolecular hydrogen bond in the lateral side chains of FQ and RQ is not present in water. In FQ and RQ a closed conformation where polar groups are masked from the solvent is formed by the establishment of a temporary ring system. In Me-FQ and Me-RQ only open conformations where the polar groups are exposed to the solvent are in evidence. The closed forms are expected to display higher membrane permeability. These results agree well with recently reported work in other systems. Specifically, similar behavior has been reported in NK1 receptor agonists[29] and cyclic peptides.[30] However, these few examples all involve six-membered rings. FQ and RQ would thus represent a new class involving a seven-membered ring. Finally, it is noteworthy that this seven-membered ring is nonplanar, whereas the six-membered ring is planar.[31] In addition, the intramolecular hydrogen bond in FQ and RQ is quite weak, allowing the flip-flop (as previously discussed between the neutral FQ/RQ and the diprotonated FQH_2^{2+} (or RQH_2^{2+})).[16] These two observations demonstrate that the molecules designed for this study completely agree with our starting hypotheses and that the comparison of their properties can enable a better understanding of the mechanism of action of FQ.

The current data suggest that replacement of the iron atom in FQ by a ruthenium atom in RQ has a small but significant effect on the physicochemical properties of the compounds, including a slight decrease in the pK_a of the terminal amino group and an increase in lipophilicity at pH 7.4. As might be expected, introduction of a methyl group on the 4-amino nitrogen atom has a much greater effect on the physicochemical properties. Both Me-FQ and Me-RQ are significantly more lipophilic than their parent compounds, FQ and RQ respectively. This is not surprising in view of the hydrophobicity of the CH_3 group. The substantial increase in pK_a of the terminal amino groups in Me-FQ and Me-RQ relative to FQ and RQ is supported by the absence of the intramolecular hydrogen bond in their structures. The increase in lipophilicity and of weak base properties in Me-FQ and Me-RQ is not associated with increased antimalarial properties, as both molecules are less active than FQ and RQ. These results agree with our previous studies where we showed that there were

no correlations between *P. falciparum* culture growth inhibition and lipophilicity of the ferrocenic compounds.[32] As a consequence, the significance of VAR in predicting the antimalarial activity of ferrocene-quinoline hybrids can be questioned.

The mechanism of action of CQ has been the subject of investigation since its introduction as a therapeutic agent but is not yet fully understood. The most probable mechanism of action involves accumulation of CQ in the malaria parasite acidic food vacuole where it inhibits hemozoin formation. Two main hypotheses coexist: (i) binding of a CQ-heme complex to the growing crystal, terminating its growth,[33] and (ii) a direct absorption of CQ to the hemozoin crystal faces.[24] Our data suggest that the mechanism of action of FQ, RQ, Me-FQ, and Me-RQ share similarities with that of CQ but also exhibit significant differences. Surprisingly, RQ showed a marked decrease in association constant with hematin and a change in stoichiometry from 1:1 for FQ:hematin to 2:1 for RQ:hematin. At first glance, we may explain the difference of association by the larger size of the ruthenium atom in comparison to the iron atom. However, if this is the reason, it is not obvious why the steric effect is not evident for Me-RQ, which forms a 1:1 complex with hematin as observed for FQ and Me-FQ. Modeling studies of the FQ-hemozoin interactions revealed that FQ is able to bind to the {0,0,1} and {1,0,0} faces of β-hematin crystal. As modeled for CQ,[25] the interacting forms of FQ are the mono- or diprotonated forms, because of the proton transfer from one (or two) propionic acid(s) of the β-hematin crystal to the basic amino group(s) of FQ. The higher fraction of neutral and monoprotonated forms of FQ relative to CQ (Table 3) may explain the higher efficiency of FQ to bind the β-hematin crystal. A similar trend is observed for RQ.

Another interesting observation is that FQ and RQ are considerably more active than CQ *in vitro*, even when tested against susceptible strains (Figure 7). Obviously, this difference may arise from improved membrane transport in relation to not only their lipophilicity but also with the presence of the intramolecular hydrogen bond in their lateral side. In contrast to FQ, RQ had no curative effect in *P. vinckei vinckei*-infected mice at 10 mg/kg/d. The apparent inhibitory activities of FQ and RQ can be misleading because most culture media do not exactly reproduce an environment relevant to infection *in vivo*. In fact, the *in vitro* cultures (especially the presence of only 10% serum in the medium) may induce, by a decrease of antioxidant buffer effect, an "external" oxidative stress in addition to the "internal" oxidative stress.

The high activity of FQ (and RQ) on CQ-, QN-, monodesethyl-AQ-, or MQ-resistant *P. falciparum* strains or isolates and the absence of cross-resistance suggest that both drugs have different modes of action and/or mechanisms of resistance. These mechanisms are different from those involved in CQ, QN, and MQ resistance, since no correlation was observed with polymorphisms in *pfcrt*, *pfmrp*, *pfmdr1*, or *pfnhe-1*. The absence of relationship between FQ activity and polymorphisms in the *pfcrt* gene is consistent with previous results.[34,35] In contrast to CQ, the presence of the ferrocene core in FQ dramatically modifies the pharmacological behavior of FQ. FQ activity is independent of CQ resistance in *P. falciparum*. FQ is able to form complexes with hematin (ratio 1:1 for both FQ and CQ) and inhibits hematin crystallization into β-hematin (IC_{50} 0.8 *versus* 1.9 for CQ). The interaction of the ferrocene core with lipid structures may allow the drug to escape the transport system involved in resistance and to concentrate at the site where the action of FQ is optimal for the inhibition of hemozoin formation.[36] In addition, FQ is able to produce significant amounts of hydroxyl radicals in the acidic and oxidizing conditions of the digestive vacuole. These radicals are very damaging for the parasite. An alternative explanation is that FQ is responsible for destruction of the hematin-drug complex by the Fenton reaction (in the conditions of the β-hematin assay). In both cases, CQ is unable to produce such a reaction, which is directly linked to the reactivity of the ferrocene *via* the generation of ferricinium ion. The high antimalarial activity of RQ suggests that the redox contribution is not essential *in vitro*, although the redox contribution may be critical *in vivo* (see above), but the higher amounts of neutral and monoprotonated forms of RQ compared to FQ (about 2-fold, Table 3) may compensate the absence of redox behavior. Our current ultrastructural studies suggest that different mechanisms of action may be involved. FQ and to a lesser extent Me-FQ appear to break down the digestive vacuole membrane, while no such effect occurs with RQ and Me-RQ. Damage to the FV membrane could originate either from reactive oxygen radicals produced by the ferrocene or from hematin that is not incorporated into hemozoin.

In contrast with FQ, we found a significant positive correlation between responses to Me-FQ and CQ. Furthermore, before Bonferroni correction, both Me-FQ and CQ showed correlations between polymorphisms in *pfcrt*, *pfmrp* and number of DNNND or DDDNHNDNHNN repeats in ms4760. These data suggest that Me-FQ and CQ have the same mechanism of resistance and are probably expelled by the same transport proteins. This process may play an important role in the molecular mechanism of action of FQ.

Previous studies with FQ and RQ suggested that the metallocene core serves only as a hydrophobic spacer group,[15,37,38] but the role of the intramolecular hydrogen bond was not taken into account. The data reported here, in addition to our previous studies,[32] clearly show that the hydrophobic effect in FQ and RQ is not sufficient to explain their remarkable antimalarial activity. The special conformation of FQ and RQ owing to their intramolecular hydrogen bond, as well as the subtle balance between their neutral, monoprotonated, and diprotonated forms allows them to cross the membranes more efficiently than CQ. Moreover, the neutral and monoprotonated species are able to interact more efficiently with the hemozoin crystal than CQ. Even if the production of OH° radicals by FQ is not the key step in *in vitro* studies, this contribution may become larger *in vivo*. Furthermore, we show that the hydrophobic effect of the lateral side chain does not play a role in the mechanisms of resistance. The interaction of the ferrocene core with lipid structures[36] may enable FQ to escape the transport system involved in resistance and to concentrate the drug at the site where its action is optimal for the inhibition of hemozoin formation. This precise mechanism needs to be investigated in detail.

Both FQ and RQ are potently active against drug-susceptible and -resistant strains of *P. falciparum*. Their levels of activity against various strains of parasite are correlated to each other but not to the activity of CQ. In addition, levels of activity do not appear to be correlated with mutations or gene copy number in any of the genes known to confer drug resistance against other quinoline antimalarials. Thus despite some significant differences in physicochemical properties, most notably their redox activities, they appear to be very similar in their activity against parasites *in vitro*. RQ is not likely to be useful as a drug because of the greater expense of Ru relative to Fe and potential toxicity associated with the heavier element. Moreover, FQ clearly demonstrated superiority over RQ *in vivo* in *P. vinckei vinckei* infected mice. Nonetheless, RQ may be a very useful analogue to

probe the cellular distribution and bioconcentration of FQ in cells. On the other hand, methylation of the 4-amino N atom of FQ and RQ reduces biological activity in both cases and substantially enhances cross-resistance with CQ in the case of Me-FQ. These findings provide important new clues to the mode of action of FQ and suggest new probes for investigation of its mode of action that may ultimately point the way to new compounds with further improved pharmacological profiles.

METHODS

General. Nuclear magnetic resonance (^{1}H, ^{13}C, and ^{15}N NMR) spectra were recorded at RT or 280 K on a Bruker Avance DPX 300 or a Bruker Avance 400 spectrometer. Deuterated chloroform (Euriso-top, Saint-Aubin, France) was used as the solvent. ^{1}H, ^{13}C, and ^{15}N NMR analyses were performed at 300 MHz (s, singlet; br s, broad singlet; d, doublet; t, triplet; dd, double doublet; m, multiplet), 75.4 and 40.6 MHz, respectively. The chemical shifts (δ) are given in parts per million relative to internal TMS ($\delta = 0.00$) for ^{1}H and ^{13}C. ^{15}N-HMBC experiments were performed using a standard sequence with a long-range coupling constant set to 8 Hz and referenced to external pure nitromethane ($\delta = 380.5$ ppm). NOESY experiments were recorded at 280 K with a 300 ms mixing time.

Mass spectra were recorded on a Waters Micromass Quattro II triple quadrupole LC mass spectrometer equipped with electrospray ionization (ESI) and atmospheric pressure chemical ionization (APCI) sources. Melting points were determined on a Köfler apparatus and are uncorrected. Column chromatography, carried out on silica gel (Merck Kieselgel 60), was used for the purification of compounds. Reactions were monitored by thin-layer chromatography (TLC) using coated silica gel plates with detection under a UV lamp.

Chemical Synthesis of 7-Chloro-4-{*N*-methyl-[2-(*N*′,*N*′-dimethylaminomethyl)-*N*-ruthenocenyl-methylamino]}-quinoline (Me-RQ). A mixture of *N*,*N*-dimethyl-1-{3-[(methylamino)methyl]ruthenocenyl}methanamine **1** (1.00 g, 3.0 mmol), 4,7-dichloroquinoline (2.96 g, 15.0 mmol), triethylamine (5.81 g, 57.3 mmol), and K_2CO_3 (1.65 g, 11.9 mmol) in *N*-methyl-2-pyrrolidone (21.0 mL) was stirred at 135 °C under N_2 for 6 h. After cooling to RT, the organic phase was extracted with citric acid solution (5%). The resulting aqueous phase was neutralized with K_2CO_3 to basic pH and extracted with dichloromethane (3×20 mL). The organic phase was washed with brine (10×20 mL) and dried over Na_2SO_4. The solvent was evaporated under reduced pressure. The crude product was purified by chromatography on a silica gel column using ethyl acetate/petroleum ether (1:1) to ethyl acetate/petroleum ether/triethylamine (5:4.5:0.5) to yield a cream solid in 25% yield: mp 146−147 °C. ^{1}H NMR (300 MHz, $CDCl_3$) 2.10 (s, 6H); 2.86 (d, $J = 13.0$ Hz, 1H); 3.02 (s, 3H); 3.17 (d, $J = 13.0$ Hz, 1H); 4.22 (d, $J = 14.7$ Hz, 1H); 4.35 (d, $J = 14.7$ Hz, 1H); 4.48 (s, 5H); 4.50 (m, 1H); 4.64 (m, 1H); 4.71 (m, 1H); 6.78 (d, $J = 5.2$ Hz, 1H); 7.36 (dd, $J = 2.0$ Hz and $J' = 2.2$ Hz, 1H); 8.01 (d, $J = 2.5$ Hz, 1H); 8.02 (d, $J = 8.8$ Hz, 1H); 8.63 (d, $J = 5.1$ Hz, 1H); ^{13}C NMR (75.4 MHz, $CDCl_3$) 40.2 (CH_2); 45.2 (CH_3); 54.1 ($2CH_3$); 57.6 (CH_2); 69.1 (CH (Cp)); 71.6 (CH (Cp′); 72.1 (CH (Cp); 73.2 (CH (Cp); 87.3 (C^{IV} (Cp); 87.4 (C^{IV} (Cp); 108.3 (CH); 121.6 (CH); 125.5 (CH); 125.9 (CH); 128.6 (C^{IV}); 134.6 (C^{IV}); 150.5 (C^{IV}); 151.4 (CH); 157.2 (C^{IV}); MS (TOF ES+) (MH^+ $^{104}Ru^{35}Cl$) 495.5; (MH^+ $^{102}Ru^{35}Cl$) 493.5; (MH^+ $^{101}Ru^{35}Cl$) 492.5; (MH^+ $^{104}Ru^{37}Cl$) 497.5; (MH^+ $^{102}Ru^{37}Cl$) 495.5; (MH^+ $^{101}Ru^{37}Cl$) 494.5. Anal. ($C_{24}H_{26}ClN_3Ru \cdot 1/2H_2O$) C, H, N.

Spin Trapping. EPR spin trapping measurements were performed according to a reported procedure (Supplementary S6).[6] EPR spectra were simulated using Winsim 2002.[39]

Computational Details. All calculations were performed with the Amsterdam Density Functional (ADF) program.[40] Molecular orbitals (MOs) were expanded using the valence triple-ζ plus polarization basis set TZVP.[19] Scalar relativistic corrections were included self-consistently using the Zeroth Order Regular Approximation (ZORA).[41] Geometries were optimized using the nonlocal generalized gradient corrected functionals (RPBE)[17,18] in singlet spin state for iron(II) and ruthenium(II). E° calculations were performed using the ORCA program.[42] The energies of the different oxidation states have been evaluated using the B3LYP[21,22] functional and TZVP basis sets. To take into account the solvent, we have used the Cosmo-rs[43] representation of water.

Interactions between the growth units were calculated using molecular mechanics. The Compass force field comes with its own charge set.[44] Most parameters were derived on the basis of *ab initio* calculations. However, the parameters were optimized empirically to yield good agreement with experimental data. In particular, thermophysical data for crystals were used to refine the nonbonded parameters by using molecular dynamics simulations. For Compass force field Cerius2 version 4.5 was used for the calculations.[45]

Partition Coefficients: log *D* (pH 7.4 and 5.2). The relative log *D* values were assessed at pH 7.4 and 5.2 by the micro-HPLC method (Supplementary S10).[23,46]

Potentiometric Titration for pK_a determination. A quantity of 5×10^{-5} mol of compound was dissolved in a mixture of 25 mL of hydrochloric acid (5×10^{-3} M) and 25 mL of dioxane. KNO_3 (0.1 M) was added to this solution to adjust the ionic strength. The solution was stirred while connected to a thermostatted water bath and allowed to equilibrate thermally. Then, the initial pH was recorded using a potentiometric glass pH meter. The solution was titrated using aliquots of a known volume of 0.01 M NaOH. The pH of the solution was measured 10 s after each addition of NaOH.

Association Constants. The spectrophotometric titration method by which association constants with Fe(III)PPIX were obtained has been previously reported (see Supporting Information for more details).[23,47] Association constants were measured in 40% (v/v) aqueous DMSO buffered at pH 7.4. This medium differs from physiological conditions both with respect to pH and the inclusion of DMSO. However, it has the advantage of maintaining hematin in a soluble and monomeric state at concentrations used[48] and has been extensively employed for investigating structure activity relationships in quinoline antimalarials (Supplementary S12).[49,23]

***Plasmodium falciparum* Cultures..** In total, 15 parasite strains (common laboratory strains or strains obtained from isolates after growth in culture for an extended period of time) from a wide panel of countries and regions (Brazil, Cambodia, Cameroon, Djibouti, the Gambia, Honduras, Indochina, Niger, Republic of Comoros, Republic of the Congo, Senegal, Sierra Leone, and Uganda)[34,50] were maintained in culture in RPMI 1640 (Invitrogen, Paisley, U.K.), supplemented with 10% human serum (Abcys S.A. Paris, France), and buffered with 25 mM HEPES and 25 mM $NaHCO_3$. Parasites were grown in type A+ human blood under controlled atmospheric conditions that consisted of 10% O_2, 5% CO_2, and 85% N_2 at 37 °C with a humidity of 95%. All strains were synchronized twice with sorbitol before use.[51] Clonality was verified using PCR genotyping of polymorphic genetic markers, msp1, msp2, and microsatellite loci.[52,53] The *in vitro* antimalarial activity for each strain was evaluated in four to nine independent experiments (Supplementary S13−S19).

Curative Effect on Mice Infected with *P. vinckei vinckei* Strains. Groups of five mice were inoculated i.p. with 10^7 parasitized erythrocytes in 0.5 mL of PBS. The first treatment dose was given subcutaneously 1 h after infection on day 0 and was repeated once daily for 3 days, as a "4-day-blood shizontocidal test".[54] Each mouse received RQ, Me-FQ, or Me-RQ dissolved in 200 μL of 0.5% methylcellulose, 0.5% Tween80 in PBS. At day 4 of infection, thin blood smears were made from mouse tail blood. They were fixed in methanol and stained with Giemsa. At least 1,000 cells were counted to determine parasitemia

and 100 fields were examined before a preparation was considered negative. Then, animals were monitored daily for death.

Toxicity Studies. The cytotoxicity of compounds was evaluated by using 3T6 fibroblast cells (kindly provided by the Laboratory of Biology and Embryology of the University of Mons-Hainaut, Supplementary S20).[55]

■ ASSOCIATED CONTENT

Supporting Information. This material is available free of charge *via* the Internet at http://pubs.acs.org.

■ AUTHOR INFORMATION

Corresponding Author

*(C.B.) Phone: +33-3-20436941. Fax: +33-3-20436555. E-mail: christophe.biot@univ-lille1.fr. (T.J.E.) Phone: +27-21-650-2528. Fax: +27-21-650-5195. E-mail: timothy.egan@uct.ac.za.

Author Contributions

T. J. Egan and C. Biot contributed equally to this work.

■ ACKNOWLEDGMENT

C.B. and F.D. would like to thank Y. Guéradel, Director of the group "Biodiversité associée aux glycoconjugués", for helping to make this study possible. This study was funded by a grant from the Ministère de l'Enseignement Supérieur to F.D. T.J.E. thanks the National Research Foundation, the Medical Research Council of South Africa. and the University of Cape Town for financial support.

■ REFERENCES

(1) www.who.int/malaria/world_malaria_report_2009/en/

(2) Eastman, R. T., and Fidock, D. A. (2009) Artemisinin-based combination therapies: a vital tool in efforts to eliminate malaria. *Nat. Rev. Microbiol. 7*, 864–874.

(3) Noedl, H., Se, Y., Schaecher, K., Smith, B. L., Socheat, D., and Fukuda, M. M. (2008) Evidence of artemisinin-resistant malaria in western Cambodia. *N. Engl. J. Med. 359*, 2619–2620.

(4) Biot, C., and Dive, D. (2010) Bioorganometallic chemistry and malaria, in *Medicinal Organometallic Chemistry* (Jaouen, G., and Metzler-Nolte, N., Eds.) Topics in Organometallic Chemistry, Vol. 32, pp 155−194, Springer, Berlin.

(5) http://clinicaltrials.gov/ct2/show/NCT00988507

(6) Chavain, N., Vezin, V., Dive, D., Touati, N., Paul, J.-F., Buisine, E., and Biot, C. (2008) Investigation of the redox behavior of ferroquine, a new antimalarial. *Mol. Pharm. 5*, 510–516.

(7) Biot, C., Chavain, N., Dubar, F., Pradines, B., Trivelli, X., Brocard, J., Forfar, I., and Dive, D. (2009) Structure−activity relationships of 4-N-substituted ferroquine analogues: Time to re-evaluate the mechanism of action of ferroquine. *J. Organomet. Chem. 694*, 845–854.

(8) Henry, M., Alibert, S., Orlandi-Pradines, E., Bogreau, H., Fusai, T., Rogier, C., Barbe, J., and Pradines, B. (2006) Chloroquine resistance reversal agents as promising antimalarial drugs. *Curr. Drug Targets 7*, 935–948.

(9) Saliba, K. J., Lehane, A. M., and Kirk, K. (2008) A polymorphic drug pump in the malaria parasite. *Mol. Microbiol. 70*, 775–779.

(10) Pradines, B., Pages, J. M., and Barbe, J. (2005) Chemosensitizers in drug transport mechanisms involved in protozoan resistance. *Curr. Drug Targets Infect. Disord. 5*, 411–431.

(11) Pradines, B. (2009) ABC proteins involved in protozoan parasites resistance, In *ABC Transporters and Multidrug Resistance* (Boumendjel, A., Boutonnat, J., and Robert, J., Eds.), pp 195−238, Wiley & Sons Inc., New York

(12) Pradines, B., Parquet, V., Orlandi-Pradines, E. (2009) ABC Transporters in *Plasmodium falciparum* and their involvement in resistance to animalarial drugs, In *ABC Transporters in Microorganisms* (Ponte-Sucre, A., Ed.), pp 113−127, Horizon Scientific Press, Norwich, U.K.

(13) Pradines, B., Pistone, T., Ezzedine, K., Briolant, S., Bertaux, L., Receveur, M. C., Parzy, D., Millet, P., Rogier, C., and Malvy, D. (2010) Quinine-resistant malaria in traveler returning from Senegal, 2007. *Emerging Infect. Dis. 16*, 546–548.

(14) Biot, C., Glorian, G., Maciejewski, L., Brocard, J., Domarle, O., Blampain, G., Millet, P., Georges, A. J., Abessolo, H., Dive, D., and Lebibi, J. (1997) Synthesis and antimalarial activity *in vitro* and *in vivo* of a new ferrocene-chloroquine analogue. *J. Med. Chem. 40*, 3715–3718.

(15) Beagley, P., Blackie, M. A. L., Chibale, K., Clarkson, C., Moss, J. R., and Smith, P. J. (2002) Synthesis and antimalarial activity *in vitro* of new ruthenocene−chloroquine analogues. *Dalton Trans. 23*, 4426–4433.

(16) Dubar, F., Khalife, J., Brocard, J., Dive, D., and Biot, C. (2008) Ferroquine, an ingenious antimalarial drug: thoughts on the mechanism of action. *Molecules 13*, 2900–2907.

(17) Perdew, J. P., Burke, K., and Ernzerhof, M. (1996) Generalized gradient approximation made simple. *Phys. Rev. Lett. 77*, 3865–3868.

(18) Hammer, B., Hansen, L. B., and Norskov, J. K. (1999) Improved adsorption energetics within density-functional theory using revised Perdew-Burke-Ernzerhof functionals. *Phys. Rev. B 59*, 7413–7421.

(19) Schäfer, A., Huber, C., and Ahlrichs, R. J. (1994) Fully optimized contracted Gaussian basis sets of triple zeta valence quality for atoms Li to Kr. *J. Chem. Phys. 100*, 5829–5835.

(20) Kannan, R., Kumar, K., Sahal, D., Kukreti, S., and Chauhan, V. S. (2005) Reaction of artemisinin with haemoglobin: implications for antimalarial activity. *Biochem. J. 385*, 409–418.

(21) Becke, A. D. (1993) Density functional thermochemistry. III. The role of exact exchange. *J. Chem. Phys. 98*, 5648–5652.

(22) Lee, C., White, D., Suits, B. H., Bancel, P. A., and Heiney, P. A. (1988) NMR study of Li in Al-Li-Cu icosahedral alloys. *Phys. Rev. B: Condens. Matter 37*, 9053–9056.

(23) Biot, C., Taramelli, D., Forfar-Bares, I., Maciejewski, L. A., Boyce, M., Nowogrocki, G., Brocard, J. S., Basilico, N., Olliaro, P., and Egan, T. J. (2005) Insights into the mechanism of action of ferroquine. Relationship between physicochemical properties and antiplasmodial activity. *Mol. Pharm. 2*, 185–193.

(24) Buller, R., Pereson, M. L., Almarsson, O., and Leiserowitz, L. (2002) Quinoline binding site on malaria pigment crystal: a rational pathway for antimalaria drug design. *Cryst. Growth Des. 2*, 553–562.

(25) Weissbuch, I., and Leiserowitz, L. (2008) Interplay between malaria, crystalline hemozoin formation, and antimalarial drug action and design. *Chem. Rev. 108*, 4899–4914.

(26) Powers, K. G., Jacobs, R. L., Good, W. C., and Koontz, L. C. (1969) *Plasmodium vinckei*: production of chloroquine-resistant strain. *Exp. Parasitol. 26*, 193–202.

(27) Delhaes, L., Abessolo, H., Biot, C., Berry, L., Delcourt, P., Maciejewski, L., Brocard, J., Camus, D., and Dive, D. (2001) *In vitro* and *in vivo* antimalarial activity of ferrochloroquine, a ferrocenyl analogue of chloroquine against chloroquine-resistant malaria parasites. *Parasitol. Res. 87*, 239–244.

(28) Swarts, J. C., Nafady, A., Roudebush, J. H., Trupia, S., and Geiger, W. E. (2009) One-electron oxidation of ruthenocene: reactions of the ruthenocenium ion in gentle electrolyte media. *Inorg. Chem. 48*, 2156–2165.

(29) Ashwood, V. A., Field, M. J., Horwell, D. C., Julien-Larose, C., Lewthwaite, R. A., McCleary, S., Pritchard, M. C., Raphy, J., and Singh, L. (2001) Utilization of an intramolecular hydrogen bond to increase the CNS penetration of an NK(1) receptor antagonist. *J. Med. Chem. 44*, 2276–2285.

(30) Rezai, T., Bock, J. E., Zhou, M. V., Kalyanaraman, C., Lokey, R. S., and Jacobson, M. P. (2006) Conformational flexibility, internal hydrogen bonding, and passive membrane permeability: successful in silico prediction of the relative permeabilities of cyclic peptides. *J. Am. Chem. Soc. 128*, 14073–14080.

(31) Kuhn, B., Mohr, P., and Stahl, M. (2010) Intramolecular hydrogen bonding in medicinal chemistry. *J. Med. Chem. 53*, 2601–2611.
(32) Biot, C., Daher, W., Ndiaye, C. M., Melnyk, P., Pradines, B., Chavain, N., Pellet, A., Fraisse, L., Pelinski, L., Jarry, C., Brocard, J., Khalife, J., Forfar-Bares, I., and Dive, D. (2006) Probing the role of the covalent linkage of ferrocene into a chloroquine template. *J. Med. Chem. 49*, 4707–4714.
(33) Sullivan, D. J., Jr., Gluzman, I. Y., Russell, D. G., and Goldberg, D. E. (1996) On the molecular mechanism of chloroquine's antimalarial action. *Proc. Natl. Acad. Sci. U.S.A. 93*, 11865–11870.
(34) Henry, M., Briolant, S., Fontaine, A., Mosnier, J., Baret, E., Amalvict, R., Fusai, T., Fraisse, L., Rogier, C., and Pradines, B. (2008) *In vitro* activity of ferroquine is independent of polymorphisms in transport protein genes implicated in quinoline resistance in *Plasmodium falciparum*. *Antimicrob. Agents Chemother. 52*, 2755–2759.
(35) Kreidenweiss, A., Kremsner, P. G., Dietz, K., and Mordmuller, B. (2006) *In vitro* activity of ferroquine (SAR97193) is independent of chloroquine resistance in *Plasmodium falciparum*. *Am. J. Trop. Med. Hyg. 75*, 1178–1181.
(36) Hoang, A. N., Ncokazi, K. K., De Villiers, K. A., Wright, D. W., and Egan, T. J. (2010) Crystallization of synthetic haemozoin (-haematin) nucleated at the surface of lipid particles. *Dalton Trans. 39*, 1235–1244.
(37) Blackie, M. A., and Chibale, K. (2008) Metallocene antimalarials: the continuing quest. *Met. Based Drugs 2008*, 495123.
(38) Kaur, K., Jain, M., Reddy, R. P., and Jain, R. (2010) Quinolines and structurally related heterocycles as antimalarials. *Eur. J. Med. Chem. 45*, 3245–3264.
(39) Duling, D. R. (1994) Simulation of multiple isotropic spin-trap EPR spectra. *J. Magn. Reson. B 104*, 105–110.
(40) Baerends, E. J. *et al.* (2005) *ADF*, 2005.01, SCM, Amsterdam.
(41) Van Lenthe, E., Baerends, E. J., and Snijders, J. G. (1993) Relativistic regular two-component Hamiltonians. *J. Chem. Phys. 99*, 4597–4610.
(42) http://www.thch.uni-bonn.de/tc/orca/
(43) Sinnecker, S., Rajendran, A., Klamt, A., Diedenhofen, M., and Neese, F. (2006) Calculation of solvent shifts on electronic g-tensors with the conductor-like screening model (COSMO) and its self-consistent generalization to real solvents (direct COSMO-RS). *J. Phys. Chem. A 110*, 2235–2245.
(44) Sun, H. (1998) COMPASS: an ab initio force-field optimized for condensed-phase applications; overview with details on alkane and benzene compounds. *J. Chem. Phys. B 102*, 7338–7364.
(45) *Cerius2*, v. 4.5 (2001) Accelrys, San Diego, CA.
(46) Pehourcq, F., Thomas, J., and Jarry, C. (2000) A Microscale HPLC method for the evaluation of actanol-water partition coefficients in a series of new 2-amino-2-oxazolines. *J. Liquid Chromatogr. Relat. Technol. 23*, 443–453.
(47) Egan, T. J., Mavuso, W. W., Ross, D. C., and Marques, H. M. (1997) Thermodynamic factors controlling the interaction of quinoline antimalarial drugs with ferriprotoporphyrin IX. *J. Inorg. Biochem. 68*, 137–145.
(48) Asher, C., de Villiers, K. A., and Egan, T. J. (2009) Speciation of ferriprotoporphyrin IX in aqueous and mixed aqueous solution is controlled by solvent identity, pH, and salt concentration. *Inorg. Chem. 48*, 7994–8003.
(49) Egan, T. J., and Ncokazi, K. K. (2004) Effects of solvent composition and ionic strength on the interaction of quinoline antimalarials with ferriprotoporphyrin IX. *J. Inorg. Biochem. 98*, 144–152.
(50) Parquet, V., Briolant, S., Torrentino-Madamet, M., Henry, M., Almeras, L., Amalvict, R., Baret, E., Fusai, T., Rogier, C., and Pradines, B. (2009) Atorvastatin is a promising partner for antimalarial drugs in treatment of *Plasmodium falciparum* malaria. *Antimicrob. Agents Chemother. 53*, 2248–2252.
(51) Lambros, C., and Vanderberg, J. P. (1979) Synchronization of *Plasmodium falciparum* erythrocytic stages in culture. *J. Parasitol. 65*, 418–420.
(52) Bogreau, H., Renaud, F., Bouchiba, H., Durand, P., Assi, S. B., Henry, M. C., Garnotel, E., Pradines, B., Fusai, T., Wade, B., Adehossi, E., Parola, P., Kamil, M. A., Puijalon, O., and Rogier, C. (2006) Genetic diversity and structure of African *Plasmodium falciparum* populations in urban and rural areas. *Am. J. Trop. Med. Hyg. 74*, 953–959.
(53) Henry, M., Diallo, I., Bordes, J., Ka, S., Pradines, B., Diatta, B., M'Baye, P. S., Sane, M., Thiam, M., Gueye, P. M., Wade, B., Touze, J. E., Debonne, J. M., Rogier, C., and Fusai, T. (2006) Urban malaria in Dakar, Senegal: chemosusceptibility and genetic diversity of *Plasmodium falciparum* isolates. *Am. J. Trop. Med. Hyg. 75*, 146–151.
(54) Peters, W. (1970) The chemotherapy of rodent malaria. X. Dynamics of drug resistance. II. Acquisition and loss of chloroquine resistance in *Plasmodium berghei* observed by continuous bioassay. *Ann. Trop. Med. Parasitol. 64*, 25–40.
(55) Mosmann, T. (1983) Rapid colorimetric assay for cellular growth and survival: application to proliferation and cytotoxicity assays. *J. Immunol. Methods 65*, 55–63.